Accepted Manuscript

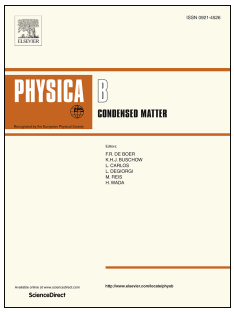

Low temperature magnetic and magnetocaloric studies in $YCr_{0.85}Mn_{0.15}O_3$ ceramic

Neeraj Panwar, Surendra Kumar, Indrani Coondoo, M. Vasundhara, Nitu Kumar

PII: S0921-4526(18)30438-1

DOI: 10.1016/j.physb.2018.06.038

Reference: PHYSB 310946

To appear in: *Physica B: Physics of Condensed Matter*

Received Date: 12 May 2018

Revised Date: 27 June 2018

Accepted Date: 28 June 2018

Please cite this article as: N. Panwar, S. Kumar, I. Coondoo, M. Vasundhara, N. Kumar, Low temperature magnetic and magnetocaloric studies in $YCr_{0.85}Mn_{0.15}O_3$ ceramic, *Physica B: Physics of Condensed Matter* (2018), doi: 10.1016/j.physb.2018.06.038.

Low temperature magnetic and magnetocaloric studies in $YCr_{0.85}Mn_{0.15}O_3$ ceramic

Neeraj Panwar[1, *], Surendra Kumar[1], Indrani Coondoo[2], M. Vasundhara[3] and Nitu Kumar[4]

[1]Department of Physics, Central University of Rajasthan, Bandarsindri, Ajmer, 305817 Rajasthan, India

[2]Department of Physics & CICECO-Aveiro Institute of Materials, University of Aveiro, 3810-193 Aveiro, Portugal

[3]Materials Science and Technology Division, CSIR-National Institute for Interdisciplinary Science and Technology, Industrial Estate, Trivandrum 695 019, India

[4]Department of Physics, University of Puerto Rico, San Juan, 00931 Puerto Rico, USA

We have investigated low temperature magnetic and magnetocaloric properties of manganese (Mn) doped $YCr_{0.85}Mn_{0.15}O_3$ (YCMO) polycrystalline compound, synthesized via solid state reaction route. The lattice volume was found to increase in comparison to that of pristine $YCrO_3$ (YCO) compound. On the other hand, the paramagnetic-antiferromagnetic Néel temperature (T_N ~ 132 K) was found to be lower than that for YCO ceramic. On cooling below T_N, under field cooled (FC) mode with an applied magnetic field of 0.02 T, magnetization flipped the polarity from positive to negative at T_{comp} = 62 K. Furthermore, the magnetization switching temperature, defined as compensation temperature, exhibited field dependency and decreased with increasing field. Besides, the magnetization reversal phenomenon disappeared under higher applied magnetic field values. For the first time, the magnetocaloric effect for this compound was

measured near 36 K through the parameters like magnetic entropy change ($-\Delta S$) = ~ 0.186 J kg^{-1} K^{-1} and the relative cooling power (RCP) ~ 6.65 J kg^{-1}, under an applied field of 5 T.

Keywords: 1. Chromites, **2.** Magnetization reversal, **3.** Magnetocaloric effect

[*]**corresponding author email:** neerajpanwar@curaj.ac.in ; neeraj.panwar@gmail.com

1. Introduction

The orthochromites ($RCrO_3$: R stands for trivalent rare-earth ion) have been extensively investigated during this decade because of their various interesting physical properties such as temperature induced magnetization reversal (TIMR) [1–3], exchange bias (EB) [3, 4], spin reorientation (SR) [3, 4] and magnetocaloric effect (MCE) [2, 5, 6]. These effects make chromites as the potential applicants for thermomagnetic switches [7], sensors [7, 8], thermally assisted random access memory [9] and magnetic refrigeration devices [10, 11]. Historically, magnetization reversal (MR, also called negative magnetization) was first observed by Néel in spinel ferrimagnetic oxides due to different temperature dependence of sublattices magnetization and their antiferromagnetic (AFM) coupling. MR is more prominently observed in $RCrO_3$ systems in comparison to orthoferrites ($RFeO_3$) or any other materials [12]. As far as MR in chromites is concerned, AFM spin order between the 3*d* electrons of Cr^{3+} ions and 4*f* electrons of R^{3+} ions is responsible for the observed behavior [3, 7-8, 13-15]. Moreover, the doping of transition metal (TM) ions like Mn^{3+} or Fe^{3+} at the Cr site also leads to the appearance of MR phenomenon. This doping induced MR in chromites is ascribed either in terms of competition between single ion anisotropy or Dzyaloshinskii-Moriya (DM) interaction and due to the paramagnetic (PM) moment of dopant ions under the negative internal field [16, 17].There are

reports of MR generation in TM doped orthochromites such as $SmCr_{0.85}Mn_{0.15}O_3$[18], $EuCr_{0.85}Mn_{0.15}O_3$[19], $LaCr_{0.85}Mn_{0.15}O_3$[16], $YCr_{1-x}Mn_xO_3$[20], $SmCr_{1-x}Fe_xO_3$[21], $LaCr_{1-x}Fe_xO3$[17], $LuCr_{1-x}Mn_xO_3$ [22], and $Sm_{0.9}Gd_{0.1}Cr_{0.85}Mn_{0.15}O_3$ [23]. Manganese ion i.e. Mn^{3+}, has one extra electron in *d*-shell in comparison to Cr^{3+} ($3d^3$) ion. This fourth electron, present in the e_g orbital, is of particular interest and is responsible for the ferromagnetic (FM) double-exchange interaction between Mn^{3+} and Cr^{3+} ions in the AFM matrix.

Compound $YCrO_3$ also comes under orthochromites even though it does not contain any rare-earth ion. It possesses orthorhombic perovskite structure with *Pnma* space group. It is reported to exhibit canted antiferromagnetism (CAFM) below the Néel temperature (T_N = 140 K) [24- 26] and dielectric anomaly like a ferroelectric transition at 473 K [27]. Recently, Mall *et al.*, through the electron paramagnetic resonance (EPR) studies and dielectric meausremnts, have suggested the presence of possible magnetodielectric coupling in $YCrO_3$ system at 230 K, much above its Néel transition temperature [28]. Experiments have also been performed to tailor its electrical, optical and magnetic properties by TM doping at Cr site. For exmpale, Sinha *et al*. [29] explored electrical and optical properties of Mn doped $YCrO_3$ nanoparticles. The optical band gap and activation energy were found to get enhanced with increasing Mn concentration. **Zhang *et al.* noticed that the electrical resistivity and activation energy increased at first and then decreased with increasing Mn content in $YCr_{1-x}Mn_xO_3$ compounds** [30]. **The ceramics exhibited the hopping conductivity and the anomaly in electrical resistivity was explained due to the variation of Cr^{4+} and Mn^{4+} ions concentration as Mn content changes.** Li *et al*. [20] explored the magnetic properties of $YCr_{1-x}Mn_xO_3$ system (x = 0.15 - 0.4). Mao *et al*. [31] demonstrated the coexistence of sign reversal of both magnetization and exchange bias in $YFe_{0.5}Cr_{0.5}O_3$ compound. Besides MR, field induced spin reorientation transition and exchange

bias have also been reported in holmium (Ho) modified $YFe_{0.5}Cr_{0.5}O_3$ compound [32, 33]. Oliveira *et al*. [6] reported MCE of $YCrO_3$ compound form 98 K to 182 K temperature range, the magnetic entropy change $(-\Delta S)$ = 0.36 $Jkg^{-1}K^{-1}$ and the refrigerant capacity or relative cooling power (RCP) = 7.1 J kg^{-1} was obtained near T_N, under an applied field of 5 T. The literature survey revealed that magnetic field dependence of magnetic properties especially magnetization reversal and the low temperature magnetocaloric effect (< 50 K) have not been performed on $YCr_{0.85}Mn_{0.15}O_3$ ceramic yet. Therefore, in this article we report such studies on$YCr_{0.85}Mn_{0.15}O_3$ compound, for the first time.

2. Experimental details

Polycrystalline $YCr_{0.85}Mn_{0.15}O_3$ (YCMO) compound was synthesized following the conventional solid state reaction method using high purity of Y_2O_3 (99.9%, Sigma Aldrich), Cr_2O_3 (99.9%, Sigma Aldrich) and MnO_2 (99.99%, Sigma Aldrich) as starting materials. Stoichiometric mixtures of these compounds were pulverized thoroughly and first calcined at 900 °C for 24 *h* followed by crushing the lump and second calcination at 1350 °C for 24 *h*. Then the products were hydrostatically pressed in the form of cylindrical pellets, and sintered in air at 1400 °C for 24 *h*. The crystal structure of samples was characterized by x-ray diffractometer (PANalytical-Empyrean) and analyzed using the Rietveld analysis program. The XRD data were recorded using Cu K_α radiation with wavelength 1.540 Å at a scanning rate of 0.01degree per second from $20° \leq \theta \leq 80°$.The surface morphology was studied by a field emission scanning electron microscope (FESEM) using Mira3TESCAN instrument. Magnetization measurements were conducted using a vibrating sample magnetometer attached with a Quantum Design Physical Property Measurement System. The protocols of warming process for zero field cool (ZFC) case, and the cooling process for field cool (FC) case were adopted for the data

acquisition. Magnetization versus magnetic field (*M-H*) data were also acquired at different temperatures between 2-74 K range for the calculation of magnetic entropy change.

3. Results and Discussion

3.1 Structural properties

Room temperature Rietveld refined (using *FullProf* program) x-ray diffraction (XRD) pattern of YCMO compound is displayed in Fig. 1(a) while the estimated lattice parameters; a = 5.5501(1) Å, b = 7.5146(2) Å and c = 5.2464(2) Å, and the goodness-of-fitting (χ^2), reliability factors, Wyckoff positions and the density value are provided in Table I. All the characteristic peaks can be indexed to an orthorhombic G-type ($a > b/\sqrt{2} > c$) structure with *Pnma* (ICSD No. 98-025-1108) space group. It can be noticed from Table I that the lattice volume of the polycrystalline YCMO ceramic is larger than that reported for undoped $YCrO_3$ (YCO) compound [4, 25]. This is attributed to the bigger size of Mn^{+3} (0.645 Å) ion as compared to Cr^{+3} (0.615 Å) ion. Further, from the lattice parameters, we calculated the octahedral bond length ($B-O$, here B stands for Cr) and tilt angles according to the Zhao formalism[34];

$$B-O = ab/4c\,, \qquad \theta = \cos^{-1}(c/a), \qquad \emptyset = \cos^{-1}(\sqrt{2}c/b) \tag{i}$$

The θ tilting results from the bending of the $< B-O-B >$ angle, while the $\emptyset$ tilting arises from the decreasing of the c and b axes. The calculated values of bond length ($B-O$), tilt angles $\theta[101]$ and $\emptyset[010]$ are found to be 1.987 Å, 19.05° and 9.12°, respectively. Mn doping resulted in the increasing of the θ tilt angle and decrease of $\emptyset$ tilt angle in comparison to the values of pristine $YCrO_3$ compound [35]. The FESEM image of sintered pellet is delineated in the Fig. 1(b). The grain growth usually takes place during sintering process and the present micrograph

revealed the polyhedral shaped polycrystalline grains of varying size. The average grain size of the compound, estimated from the grain size distribution histogram using Microsoft Visio-2013 software, was 373 nm [inset Fig. 1(b)]. The stoichiometric ratios of the constituents of YCMO compound was confirmed by Energy-dispersive X-ray spectroscopy (EDXS) and the same is illustrated in Fig. 1(c).The presence of subtle amount of aluminum (Al) in the EDXS image may be from the alumina (Al_2O_3) crucible, which was used for the preparation of the compound.

Table I: List of reliability factors and atomic positions from the Rietveld refinement.

Reliability factors					
χ^2	R_F	R_{wp}	R_P	Volume(Å^3)	Density (g/cm^3)
2.18	3.57%	12.9%	16.5%	218.8105	5.595

Atomic positions					
	Wyckoff positions	x	y	z	Occ.
Y	4c	0.0681(4)	0.25	0.0181(5)	0.9691
Cr	4b	0	0	0.5	0.8056
Mn	4b	0	0	0.5	0.1502
O1	4c	-0.035(3)	0.25	0.595(2)	0.8660
O2	8d	é0.711(1)	-0.054(2)	0.301(2)	1.7789

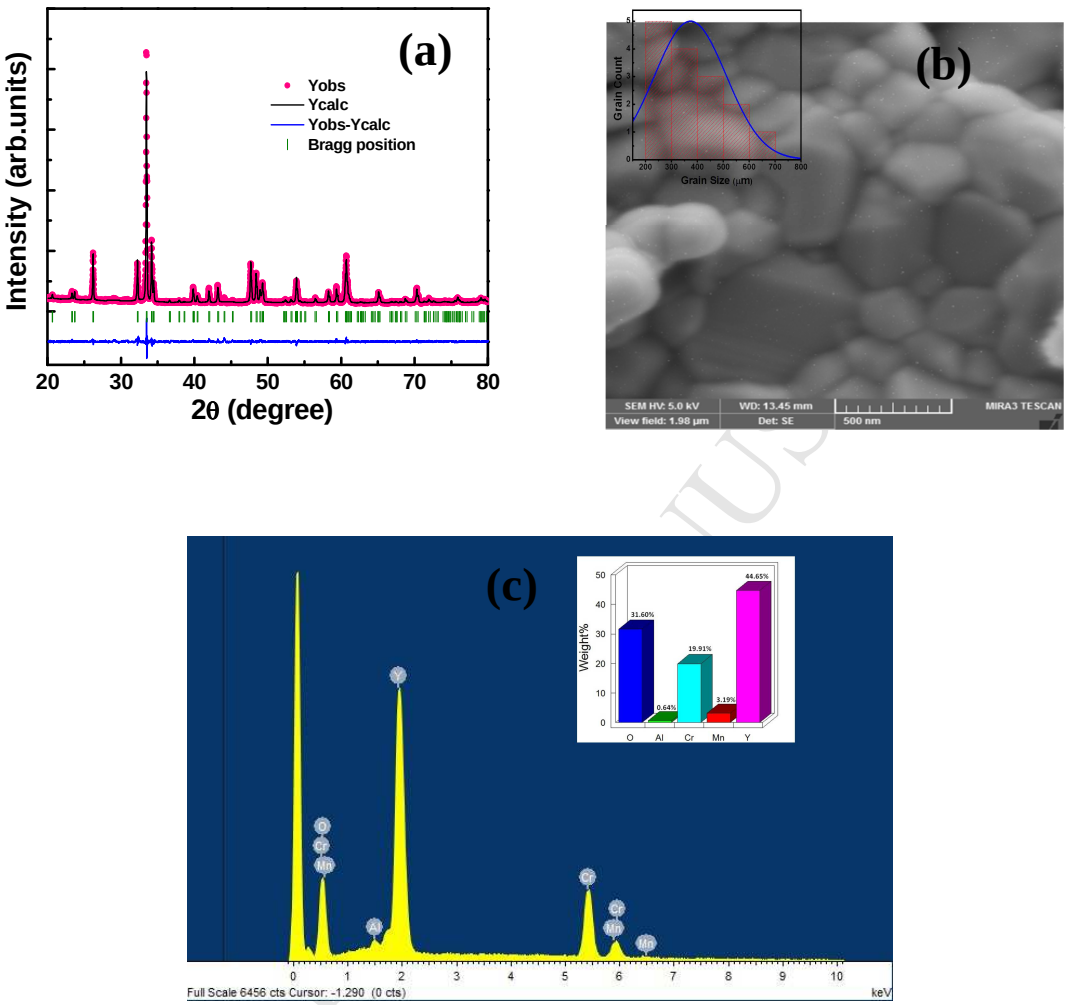

Figure 1: (**a**) XRD pattern, (**b**) FESEM micrograph and (**c**) EDXS image of YCMO ceramic.

3.2 Magnetic Properties:-

Fig. 2(a) displays the ZFC and FC magnetization versus temperature (*M*-*T*) curves of YCMO compound at an applied field of 0.02 T in a temperature range from 2 to 300 K. From

room temperature to Néel temperature T_N ~ 132 K [calculated from the derivative of magnetization and shown in inset of Fig. 2(a)] the sample exhibited the paramagnetic behavior. It is worth mentioning here that T_N for the pristine $YCrO_3$ is ~141 K **[4, 24-25]**.The T_N of YCMO sample decreased with respect to that of pristine YCO because of the development of double-exchange interaction between Mn^{4+}/Cr^{3+} and Mn^{3+} ions [18–20, 36]. **The itinerant electron of Mn^{3+} ($t_{2g}^3 e_g^1$) ion hops between Mn^{3+} and Mn^{4+}/Cr^{3+} ($t_{2g}^3 e_g^0$) through oxygen ion. This mechanism leads to the development of the ferromagnetic (FM) behavior and the weakening of the antiferromagnetic interaction among Cr^{3+} ions and the ensuing decrease in Néel temperature.**

Further, in order to get more insight about the magnetic behavior of the present compound, we plotted reciprocal of magnetic susceptibility χ^{-1} versus T curve (inset Fig. 2(a)). In the high temperature region (above 150 K), χ^{-1} behaves linearly and well fitted by the Curie-Weiss law as shown by the solid line. From the fitting, the calculated effective magnetic moment (μ_{eff}) and asymptotic paramagnetic Curie temperature (θ_W) are found to be 4.6 μ_B/f.u. and - 242 K, respectively. **The theoretically obtained negative value of θ_W (though experimentally no temperature exists below 0 K) signifies the antiferromagnetic interaction among the Cr^{3+} ions [6]. Had it been a ferromagnetic interaction, the sign of θ_W would have been positive**. The estimated theoretical value from $\mu_{eff}(cal) = \sqrt{x(\mu_{eff}^{Mn})^2 + (1-x)(\mu_{eff}^{Cr})^2}$ was 4.04 μ_B/f.u. which is due to the contribution of a spin-only Cr^{3+} and a free-ion Mn^{3+} moment. It is satisfying to note that the theoretical and experimental values are close to each other.

Below T_N in both ZFC and FC mode (under H = 0.02 T), magnetization increases with decreasing temperature. The M_{FC} curve develops a hump with peak at T_{peak} = 102 K and

magnetization maximum M_{max} ~ 0.26 emu/g. Thereafter, it decreases monotonously crosses zero magnetization (M_{FC} = 0) at compensation temperature T_{comp} ~ 62 K. Finally, M_{FC} approaches a minimum value of M_{min} ~ -1.09 emu/g at 2 K. On the other hand, M_{ZFC} remains almost constant up to ~ 60 K. Below this temperature, M_{ZFC} decreases rapidly. The subtle difference in the crossover temperatures between ZFC and FC data may be ascribed to the random distribution of net moments in the ZFC mode and their preferred orientation along the external field in FC mode. Like other Mn doped chromites, in present system, the magnetization reversal resulted from an interplay of different interactions such as Mn^{3+}- Mn^{3+}, Mn^{3+}- Cr^{3+} and Cr^{3+}- Cr^{3+} which are either FM or AFM in nature [20]. The amount of magnetization reversal is usually measured in terms of the ratio of M_{Min} and M_{Max}, *i.e.* M_{Min}/M_{Max}, and for the present studied compound it is found to be ~ - 4.2 at H = 0.02 T. Its value reported in literature for other chromites like $LaCr_{0.85}Mn_{0.15}O_3$ and $EuCr_{0.85}Mn_{0.15}O_3$ compounds, is -2 and -0.6, respectively under the same field condition [16, 19]. The crossover temperature was also found to decrease with increasing field. Further, there is an anomaly observed at 36 K in ZFC magnetization under 0.1 T applied magnetic field. This anomaly temperature is defined as spin reorientation transition, T_{SR}. At this temperature, magnetization changes slope and it is believed that the spins of Cr^{3+}ions which are coupled AFM rotate from the Γ_4 (*c-axis*) to the Γ_2 (*a-axis*). **Mn^{3+} ion is found to induce such rotation of spins in chromites** [19] **since it is a highly magnetic anisotropic Jahn Teller active ion. Therefore, the magnetic interaction energy in systems with Mn^{3+} ion consists of isotropic Heisenberg exchange term, the antisymmetric Dzyloshinskii-Moriya (DM) interaction and the last term due to magnetocrystalline anisotropy energy. In compounds like the present one where a highly magnetic anisotropic ion is present, the last term**

dominates over others and causes a decrease in magnetic energy and the ensuing spin reorientation transition.

In order to further understand the magnetization reversal, FC magnetization curves at 0.02 and 0.1 T, respectively were fitted (shown by solid line) using the following equation [14]:

$$M = M_{Cr} + \frac{C(H_I+H)}{T-\theta} \qquad \text{(ii)}$$

where M, M_{Cr}, C, H_I, H and θ stand for the total magnetization, weak FM component of canted Cr^{3+} ions, a Curie constant, an internal field from Cr^{3+} ion, an applied field and a Weiss temperature, respectively. The evaluated parameters are shown in Table II. The negative value of H_I confirms the assumption that it is opposite to the applied field and its value being larger than the applied magnetic field allows the spins of ions to get aligned antiparallel to Cr^{3+} ions. The size of AFM domains is expected to increase with increasing applied field and that gives rise to increase in H_I and M_{Cr} values. With the application of much higher applied field *i.e.*, $H \geq 0.2$ T, M_{FC} curves shift towards positive magnetization axis without any considerable change in *M-T* behavior, as shown in Fig. 2(c). This is due to the evolution of AFM domains size during increasing the applied field.

Table II: Fitting parameters for *M-T* curves recorded in FC mode.

External field (Tesla)	M_{Cr} **(emu/g)**	H_I **(Tesla)**	θ **(K)**
0.02	1.242	-0.0468	-43
0.10	1.336	-0.1303	-91

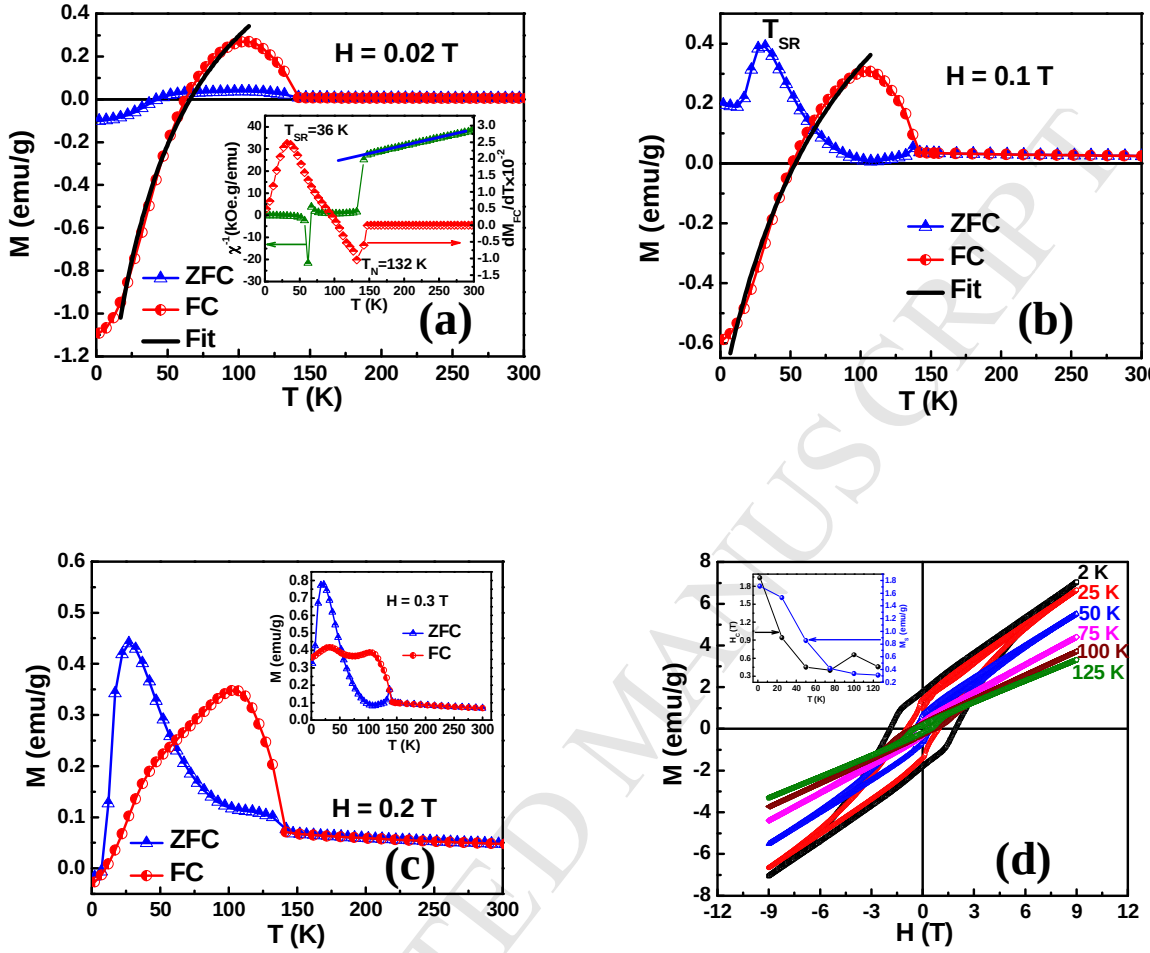

Figure2: (a)-(c) ZFC and FC magnetization curves measured at 0.02 T, 0.1 T, 0.2 T and 0.3 T. FC data fitted at 0.02 T and 0.1 T with Eq. (ii). Inset of fig. 2(a) is the reciprocal of dc magnetic

susceptibility χ^{-1} versus temperature (the solid line represents a Curie Weiss-type fit) along with dM/dT graph, **(d)** magnetization versus magnetic field at different temperatures and the temperature dependence of the saturation magnetization and the coercivity H_c of the weak FM component are shown in the inset of fig. 2(d).

In order to understand the magnetic behavior below T_N, we have acquired magnetization isotherms *M(H)* at different temperatures 2 K, 25 K, 50 K, 75 K, 100 K and 125 K in the range of ± 9 T magnetic field. The data are plotted in Fig. 2(d), from where it can be inferred that the loops are well symmetric about the field axis and exhibit hysteresis without any saturation. These loops are attributed to the coexistence of weak FM (low field) and AFM (high field) components where magnetization increases linearly in the larger magnetic field region, and the net magnetization is thus given by the relation [24] $M(H) = \chi_{AF}H+M_s$, where $\chi_{AF}H$ is the antiferromagnetic contribution and M_s is the saturation magnetization of the weak ferromagnetism. Thus the value of M_s can be obtained by subtracting the antiferromagnetic contribution from the total magnetization. Inset of Fig. 2(d) shows the decreasing trend of M_s and coercive field (H_C) values with increasing temperature up to 125 K. Chromites, like the present one, exhibit hysteresis in the magnetization temperature behavior. The area under the hysteresis curve represents the losses. This eventually abates the cooling efficiency. Such problems of chromites can be overcome by synthesizing them using any procedure that produces particle size less than 100 nm.

3.3 Magnetocaloric Property:

Magnetocaloric effect (MCE) is related to the magnetic refrigeration, it is induced via the coupling of the magnetic sublattice with the magnetic field. The magnetic entropy change (ΔS) associated with the MCE, can be evaluated from the magnetization data using the Maxwell relation [37];

$$\Delta S(T)_{\Delta H} = \int_{H_I}^{H_F} \left(\frac{\partial M(T,H)}{\partial T}\right)_H dH \qquad \text{(iii)}$$

where H_I and H_F are the initial and final applied magnetic fields, respectively. Generally, ΔS is calculated from the *M-H* curves acquired in the first quadrant. Next, equation (iii) can be simplified using trapezoidal rule [38];

$$\Delta S(T_{av})_{\Delta H} = \frac{\delta H}{2\delta T}\left(\delta M_1 + 2\sum_{i=2}^{n-1}\delta M_i + \delta M_n\right) \qquad \text{(iv)}$$

The relative cooling power (RCP) is usually calculated by integrating the magnetic entropy change between temperatures T_1 and T_2 at different magnetic field values [39];

$$RCP = \int_{T_1}^{T_2} \Delta S(T)_{\Delta H}\, dT \qquad \text{(v)}$$

where T_1 and T_2 are the low and high temperature limits in the refrigeration cycle.

In order to calculate the magnetocaloric effect for YCMO compound, *M*(*H*) data were obtained between 2-74 K temperature range with an interval of ΔT = 5 K under the magnetic field (ΔH) variation from 0-9 T. The results are plotted in Fig. 3(a). Thereafter, $-\Delta S$ versus temperature for different ΔH values was derived from the M-H curves using equation (iv). Fig. 3(b) illustrates the result of magnetic entropy change. It can be seen that $-\Delta S$ is positive in the entire temperature range with value ~ 0.186 J kg^{-1} K^{-1} observed near T_{SR} under 5 T applied magnetic field. This value is significantly smaller than that observed for chromites with magnetic rare-earth ions [36]. Nevertheless, it is comparable to chromites having nonmagnetic ions at the rare-earth site like $SmCrO_3$ (0.25J kg^{-1} K^{-1}) and $EuCr_{0.85}Mn_{0.15}O_3$ (1.82J kg^{-1} K^{-1}) under the same field

conditions [40, 19]. The RCP values was estimated from Eq. (v) with integration temperatures T_1 = 14 K and T_2 = 62 K. The maximum RCP is obtained 6.65 J kg^{-1} at H = 5 T magnetic field. The values of $-\Delta S$ and RCP at other fields are given in Table III. Although, Li *et al*. [20] have reported the magnetocaloric data of $YCr_{1-x}Mn_xO_3$ system (x = 0.15 - 0.4), however; their temperature range of study was above 70 K. Apparently, no data was available in literature at low temperature range for doped or undoped YCO compound to compare with the present compound, therefore; this is the first magnetocaloric data on doped $YCrO_3$ ceramic below 50 K.

Table III: Magnetic entropy change and relative cooling power at various applied magnetic field.

H_{Max} (T)	$-\Delta S_{Max}$ (J kg^{-1} K^{-1})	RCP (J kg^{-1})
1	0.02	1.05
3	0.102	3.66
5	0.186	6.65
7	0.273	9.87
9	0.365	13.52

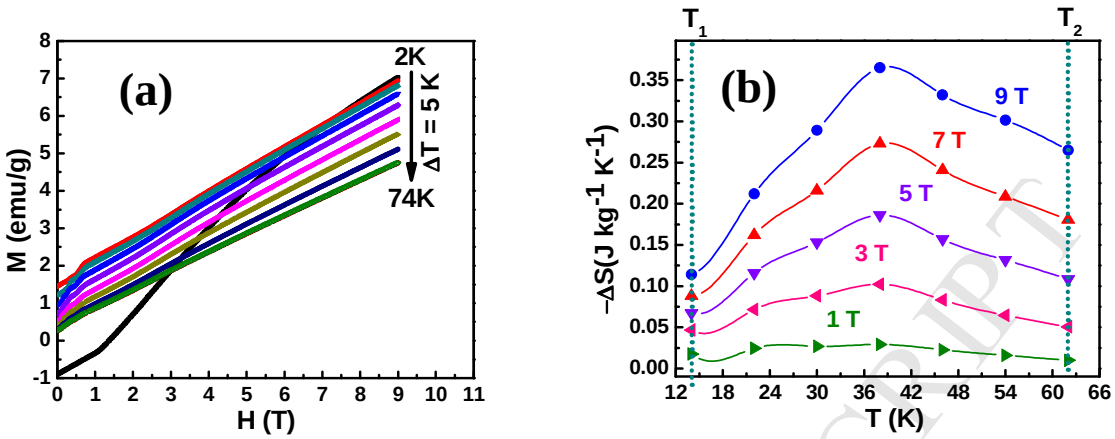

Figure 3: (**a**) *M- H* curves in first quadrant at different temperatures, (**b**) magnetic entropy change as a function of temperature under different magnetic field values.

Conclusion

In summary, we have carried out detailed low temperature investigations of magnetic and magnetocaloric properties of YCMO orthochromite. Below Néel temperature and under low applied magnetic field, magnetization reversal was observed in the FC magnetization curve which disappears with high magnetic field. Spin reorientation transition was observed and the magnetocaloric effect perceived through indirect measurement of magnetic entropy change and the relative cooling power, for the first time, exhibited maximum value near the spin reorientation temperature.

Acknowledgement

The author S. Kumar would like to thank the University Grant Commission, New Delhi, for providing the Rajiv Gandhi National Fellowship (RGNF). M. Vasundhara would also like to

thank Board of Research in Nuclear Sciences, sponsored project no. GAP 218939 for partially supporting this work.

Reference

[1] K. Yoshii and a. Nakamura, "Reversal of Magnetization in $La_{0.5}Pr_{0.5}CrO_3$," *J. Solid State Chem.*, vol. 155, no. 2, pp. 447–450, 2000.

[2] K. Yoshii, "Magnetization reversal in $TmCrO_3$," *Mater. Res. Bull.*, vol. 47, no. 11, pp. 3243–3248, 2012.

[3] P. Gupta, R. Bhargava, and P. Poddar, "Colossal increase in negative magnetization, exchange bias and coercivity in samarium chromite due to a strong coupling between Sm^{3+}–Cr^{3+} spins sublattices," *J. Phys. D. Appl. Phys.*, vol. 48, no. July 2015, pp. 25004, 2015.

[4] S. Kumar, I. Coondoo, A. Rao, B.-H. Lu, Y.-K. Kuo, A. L. Kholkin, and N. Panwar, "Impact of low level praseodymium substitution on the magnetic properties of $YCrO_3$ orthochromites," *Phys. B Condens. Matter*, vol. 510, no. January, pp. 104–108, 2017.

[5] S. Yin, T. Sauyet, M. S. Seehra, and M. Jain, "Particle size dependence of the magnetic and magneto-caloric properties of $HoCrO_3$," *J. Appl. Phys.*, vol. 121, no. 6, p. 63902, 2017.

[6] G. N. P. Oliveira, P. MacHado, A. L. Pires, A. M. Pereira, J. P. Araujo, and A. M. L. Lopes, "Magnetocaloric effect and refrigerant capacity in polycrystalline $YCrO_3$," *J. Phys. Chem. Solids*, vol. 91, pp. 182–188, 2016.

[7] Y. Cao, S. Cao, W. Ren, Z. Feng, S. Yuan, B. Kang, B. Lu, and J. Zhang, "Magnetization

switching of rare earth orthochromite $CeCrO_3$," *Appl. Phys. Lett.*, vol. 104, no. 23, pp. 1–5, 2014.

[8] P. Gupta and P. Poddar, "Temperature and Magnetic Field-Assisted Switching of Magnetization and Observation of Exchange Bias in $YbCrO_3$ Nanocrystals," *Inorg. Chem.*, vol. 54, no. 19, pp. 9509–9516, 2015.

[9] S. Bandiera and B. Dieny, "Thermally assisted MRAM," *Handb. Spintron.*, vol. 165218, pp. 1065–1100, 2015.

[10] S. Yin and M. Jain, "Enhancement in magnetocaloric properties of holmium chromite by gadolinium substitution," *J. Appl. Phys.*, vol. 120, no. 4, pp. 0–8, 2016.

[11] A. M. Tishin and Y. I. Spichkin, *The Magnetocaloric Effect and its Applications*. Institute of Physics Publishing, 2003.

[12] A. Kumar and S. M. Yusuf, "The phenomenon of negative magnetization and its implications," *Phys. Rep.*, vol. 556, pp. 1–34, 2015.

[13] L. Wang, G. H. Rao, X. Zhang, L. L. Zhang, S. W. Wang, and Q. R. Yao, "Reversals of magnetization and exchange-bias in perovskite chromite $TmCrO_3$," *Ceram. Int.*, vol. 42, no. 8, pp. 10171–10174, 2016.

[14] A. H. Cooke, D. M. Martin, and M. R. Wells, "Magnetic interactions in gadolinium orthochromite, $GdCrO_3$," *J. Phys. C Solid State Phys.*, vol. 7, no. 17, pp. 3133–3144, 1974.

[15] K. Yoshii, "Positive exchange bias from magnetization reversal in $La_{1-x}Pr_xCrO_3$ ($x \sim 0.7$–0.85)," *Appl. Phys. Lett.*, vol. 99, no. 14, pp. 142501, 2011.

[16] T. Bora and S. Ravi, "Sign reversal of magnetization and echange bias field in $LaCr_{0.85}Mn_{0.15}O_3$," *J. Appl. Phys.*, vol. 114, pp. 183902, 2013.

[17] T. Bora and S. Ravi, "Study of magnetization reversal in $LaCr_{1-x}Fe_xO_3$ compounds," *J. Appl. Phys.*, vol. 114, no. 3, pp. 33906, 2013.

[18] S. Kumar, I. Coondoo, M. Vasundhara, A. K. Patra, A. L. Kholkin, and N. Panwar, "Magnetization reversal behavior and magnetocaloric effect in $SmCr_{0.85}Mn_{0.15}O_3$ chromites," *J. Appl. Phys.*, vol. 121, no. 4, pp. 43907, 2017.

[19] S. Kumar, I. Coondoo, M. Vasundhara, V. S. Puli, and N. Panwar, "Observation of magnetization reversal and magnetocaloric effect in manganese modified $EuCrO_3$ orthochromites," *Phys. B Condens. Matter*, vol. 519, no. May, pp. 69–75, 2017.

[20] C. L. Li, S. Huang, X. X. Li, C. M. Zhu, G. Zerihun, C. Y. Yin, C. L. Lu, and S. L. Yuan, "Negative magnetization induced by Mn doping in $YCrO_3$," *J. Magn. Magn. Mater.*, vol. 432, pp. 77–81, 2017.

[21] L. H. Yin, Y. Liu, S. G. Tan, B. C. Zhao, J. M. Dai, W. H. Song, and Y. P. Sun, "Multiple temperature-induced magnetization reversals in $SmCr_{1-x}Fe_xO_3$ system," *Mater. Res. Bull.*, vol. 48, no. 10, pp. 4016–4021, 2013.

[22] D.-X. Fu, Y.-Z. Liu, H.-G. Zhang, L. Xie, and B. Li, "The evolution of magnetization switching of $LuCrO_3$by the effect of Mn doping," *J. Alloys Compd.*, vol. 735, pp. 1052–1062, 2018.

[23] N. Panwar, J. P. Joby, S. Kumar, I. Coondoo, M. Vasundhara, N. Kumar, R. Palai, R. Singhal, and R. S. Katiyar "Observation of Magnetization reversal behavior in

$Sm_{0.9}Gd_{0.1}Cr_{0.85}Mn_{0.15}O_3$ orthochromites," *AIP Adavance*, vol. 8, p. 55818, 2017.

[24] A. Durn, A. M. Arvalo-Lpez, E. Castillo-Martnez, M. Garca-Guaderrama, E. Moran, M. P. Cruz, F. Fernndez, and M. A. Alario-Franco, "Magneto-thermal and dielectric properties of biferroic $YCrO_3$ prepared by combustion synthesis," *J. Solid State Chem.*, vol. 183, no. 8, pp. 1863–1871, 2010.

[25] B. Tiwari, M. K. Surendra, and M. S. Ramachandra Rao, "$HoCrO_3$ and $YCrO_3$: a comparative study," *J. Phys. Condens. Matter*, vol. 25, no. 21, p. 216004, 2013.

[26] Y. Sharma, S. Sahoo, W. Perez, S. Mukherjee, R. Gupta, A. Garg, R. Chatterjee, and R. S. Katiyar, "Phonons and magnetic excitation correlations in weak ferromagnetic $YCrO_3$," *J. Appl. Phys.*, vol. 115, no. 18, pp. 0–9, 2014.

[27] C. R. Serrao, A. K. Kundu, S. B. Krupanidhi, U. V. Waghmare, and C. N. R. Rao, "Biferroic $YCrO_3$," *Phys. Rev. B - Condens. Matter Mater. Phys.*, vol. 72, no. 22, pp. 2–5, 2005.

[28] A. K. Mall, A. Dixit, A. Garg and R. Gupta, "Temperature dependent electron paramagnetic resonance study on magnetoelectric $YCrO_3$", *J. Phys.: Condens. Matter*vol. 29 495805, 2017.

[29] R. Sinha, S. Basu, and A. K. Meikap, "Investigation of dielectric and electrical behavior of Mn doped $YCrO_3$ nanoparticles synthesized by the sol gel method," *Phys. E Low-Dimensional Syst. Nanostructures*, vol. 69, pp. 47–55, 2015.

[30] B. Zhang, Q. Zhao, A. Chang, Y. Li, Y. Liu, and Y. Wu, " Electrical conductivity anomaly and X-ray photoelectron spectroscopy investigation of $YCr_{1-x}Mn_xO_3$ negative

temperature coefficient ceramics," *Appl. Phys. Lett.* vol.104, pp.102109 (1-4), 2014.

[31] J. Mao, Y. Sui, X. Zhang, X. Wang, Y. Su, Z. Liu, Y. Wang, R. Zhu, Y. Wang, W. Liu, and X. Liu, "Tunable exchange bias effects in perovskite $YFe_{0.5}Cr_{0.5}O_3$," *Solid State Commun.*, vol. 151, no. 24, pp. 1982–1985, 2011.

[32] L. R. Shi, Z. C. Xia, M. Wei, Z. Jin, C. Shang, J. W. Huang, B. R. Chen, Z. W. Ouyang, S. Huang, and G. L. Xiao, "Unusual effects of Ho^{3+} ion on magnetic properties of $YFe_{0.5}Cr_{0.5}O_3$," *Ceram. Int.*, vol. 41, pp. 13455–13460, 2015.

[33] L. R. Shi, C. X. Wei, Z. Wang, L. Ju, T. S. Xu, T. X. Li, X. W. Yan, and Z. C. Xia, "Positive and negative exchange bias effects from magnetization reversal in Ho^{3+} doped $YFe_{0.5}Cr_{0.5}O_3$," *J. Magn. Magn. Mater.*, vol. 433, pp. 104–108, 2017.

[34] Y. Zhao, D. J. Weidner, J. B. Parise, and D. E. Cox, "Thermal expansion and structural distortion of perovskite - data for $NaMgF_3$ perovskite. Part I," *Phys. Earth Planet. Inter.*, vol. 76, no. 1–2, pp. 1–16, 1993.

[35] M. C. Weber, J. Kreisel, P. A. Thomas, M. Newton, K. Sardar, and R. I. Walton, "Phonon Raman scattering of $RCrO_3$ perovskites (R=Y, La, Pr, Sm, Gd, Dy, Ho, Yb, Lu)," *Phys. Rev. B - Condens. Matter Mater. Phys.*, vol. 85, no. 5, pp. 1–9, 2012.

[36] S. Kumar, I. Coondoo, M. Vasundhara, S. Kumar, A. L. Kholkin, and N. Panwar, "Structural , magnetic , magnetocaloric and specific heat investigations on Mn doped $PrCrO_3$ orthochromites," *J. Phys. Condens. Matter*, vol. 29, p. 195802, 2017.

[37] A. H. Morrish, *The Physical Principles of Magnetism*, vol. 1, no. 1. 1965.

[38] V. K. Pecharsky and K. a. Gschneidner, "Magnetocaloric effect from indirect

measurements: Magnetization and heat capacity," *J. Appl. Phys.*, vol. 86, no. 1, p. 565, 1999.

[39] K. A. Gschneidner Jr., V. K. Pecharsky, A. O. Pecharsky, and C. B. Zimm, "Recent Developments in Magnetic Refrigeration," *Mater. Sci. Forum*, vol. 315–317, pp. 69–76, 1999.

[40] P. Gupta and P. Poddar, "Study of magnetic and thermal properties of $SmCrO_3$ polycrystallites," *RSC Adv.*, vol. 6, no. 85, pp. 82014–82023, 2016.